



## Evaluation of local tumor residue after percutaneous radiofrequency ablation therapy for hepatocellular carcinoma

Jun Hamanaka<sup>1,2</sup>, Tohru Goto<sup>2</sup>, Shuhei Nishigori<sup>1,2</sup>, Shihoko Seki<sup>2</sup>, Tomonori Ida<sup>2</sup>, Taiki Morohashi<sup>2</sup>, Hiroshi Ohara<sup>2</sup>, Masahiko Inamori<sup>3</sup>, Shin Maeda<sup>3</sup>

<sup>1</sup>Department of Gastroenterology, Yokohama Minami Kyosai Hospital, Yokohama, Japan

<sup>2</sup>Department of Gastroenterology, Omori Red Cross Hospital, Tokyo, Japan

<sup>3</sup>Department of Gastroenterology, Yokohama City University Hospital, Yokohama, Japan

### ABSTRACT

**Background/Aims:** This study's purpose was to compare the efficacy of CO<sub>2</sub>-enhanced ultrasonography (US) with that of Sonazoid-enhanced US and conventional US in detecting local tumor residue after percutaneous radiofrequency (RF) ablation therapy for hepatocellular carcinoma.

**Materials and Methods:** Between February 2009 and March 2010, 141 lesions of 121 hepatocellular carcinoma patients were treated by percutaneous RF ablation, and 22 tumor residues were detected in 22 patients by contrast-enhanced computed tomography. These 22 patients were examined by conventional US, Sonazoid-enhanced US (0.5 mL/body of Sonazoid, intravenous administration), and CO<sub>2</sub>-enhanced US (10 mL of CO<sub>2</sub>, hepatic arterial administration).

**Results:** Tumor residue was confirmed by CO<sub>2</sub>-enhanced US in all the 22 patients (sensitivity: 100%) in 19 of the 22 patients by Sonazoid-enhanced US (sensitivity: 86%; 3 lesions that were not detected by this modality were located deeper than the sonographic depth (p=0.0109)), and in 17 of the 22 patients by conventional US (sensitivity: 77%; 5 lesions that were not detected by this modality were smaller in terms of the sonographic tumor size (p=0.0278)).

**Conclusion:** Although CO<sub>2</sub>-enhanced US requires angiography, it was superior to both Sonazoid-enhanced US and conventional US for detecting tumor residues, particularly deep-seated ones, after percutaneous RF ablation.

**Keywords:** Hepatocellular carcinoma, computed tomography, radiofrequency ablation, Sonazoid, CO<sub>2</sub>-enhanced ultrasonography

### INTRODUCTION

Hepatocellular carcinoma is the third leading cause of mortality worldwide, often occurring in liver cirrhosis patients (1). Nearly 4 million Americans suffer from hepatocellular carcinoma, and the prevalence of this disease is on the increase in the United States. The incidence of hepatitis C virus infections has increased because of intravenous drug use (1,2).

It has been reported that surgery is the only curative effective treatment modality for hepatocellular carcinoma (3). However, in most patients with hepatocellular carcinoma, the presence of liver dysfunction caused by liver cirrhosis limits the possibility of surgical resection.

Percutaneous radiofrequency (RF) ablation therapy has recently been established as a promising local therapeutic technique for hepatocellular carcinoma in such patients (4).

In most cases, local tumor residue after RF ablation can be detected by contrast-enhanced computed tomography (CT). On the other hand, this is sometimes difficult to detect by conventional ultrasonography (US). A local residual tumor after percutaneous therapy is particularly difficult to detect because the margin between viable and necrotic tumor tissue is unclear in most cases. To improve the sensitivity of detection, contrast-enhanced US techniques have been developed. Mat-

**Address for Correspondence:** Jun Hamanaka and Masahiko Inamori E-mail: inamorim@yokohama-cu.ac.jp - j\_hamanaka@hotmail.com

**Received:** November 7, 2016 **Accepted:** February 1, 2017 **Available Online Date:** March 15, 2017

© Copyright 2017 by The Turkish Society of Gastroenterology • Available online at www.turkjgastroenterol.org • DOI: 10.5152/tjg.2017.16641

suda and Yabuuchi developed the CO<sub>2</sub>-enhanced sonography technique, which involves the injection of CO<sub>2</sub> microbubbles into the hepatic artery (5). Levovist\*, a first-generation US contrast agent, improved the localization of sonographically unrecognized hypervascular lesions of the liver (6-10). Sonazoid\*, a second-generation contrast agent composed of a hard shell containing bubbles, produces stable nonlinear oscillations in the low-power acoustic field and yields enhanced real-time details of the second harmonic signals (11,12).

The aim of our study was to compare the efficacy of CO<sub>2</sub>-enhanced US with that of Sonazoid-enhanced US and conventional US in detecting local tumor residue after percutaneous RF ablation therapy for hepatocellular carcinoma.

## MATERIALS AND METHODS

### Patients

Between February 2009 and March 2010, 141 lesions of 121 consecutive hepatocellular carcinoma patients were treated by percutaneous RF ablation in our institute. Conventional sonographic examinations and contrast-enhanced CT were performed at intervals of every 3 months post RF ablation. In the case of suspected tumor residues, Sonazoid-enhanced US and CO<sub>2</sub>-enhanced US were also performed. Tumor residues were detected by contrast-enhanced CT obtained after percutaneous RF ablation in 22 patients. These 22 patients (16 men and 6 women; age range: 49-85 years; mean: 74 years) with local tumor residues were enrolled in this study. Written informed consent was obtained from all the patients after fully explaining the nature and purpose of the study.

### Percutaneous RF Ablation

In all the patients, either the lesions were deemed inoperable or the patients had refused surgical intervention. The technique of percutaneous RF ablation has been described previously (13-16). We used the RTC 3000 or RTC 2000 systems (Boston Scientific Inc.; Natick, MA) and the Cool-tip RF ablation system (Covidien, Boulder, CO) for treating hepatocellular carcinoma patients. RF ablation was carried out under US guidance in all the patients.

### CO<sub>2</sub>-Enhanced US

CO<sub>2</sub>-enhanced sonography (5,17) was performed after angiography. We used Pro-Sound SSD-5000 (Aloka, Tokyo, Japan) with a special convex. This convex probe had a range of 2.0-3.0 MHz. The CO<sub>2</sub>-enhanced sonography was performed after hepatic angiography. CO<sub>2</sub> microbubbles were made by mixing. The composition was as follows: 10 mL of CO<sub>2</sub>, 7 mL of saline, small amount of heparin, and 3 mL of the patient's own blood. First, the CO<sub>2</sub> microbubbles were manually injected into the catheter positioned in the left or right hepatic artery; thereafter, using a real-time convex scanner with 3.5-MHz probes, we observed the flow of CO<sub>2</sub> gas and enhancement of the area of interest.

### Sonazoid-Enhanced US

Sonazoid-enhanced US (11,12) was performed in all the patients by two sonographers. The US was carried out with an Aplio XG (Toshiba, Tokyo, Japan) with a micro-convex probe (PVT-375BT, 3.5 MHz; Toshiba). We used the contrast harmonic imaging mode (pulse subtraction harmonic). The acoustic power of US was controlled at a mechanical index of 0.2-0.25. A single focus point was configured at the space occupied by the lesion. Sonazoid (0.5 mL/body) was injected via the cubital vein, and 10 mL normal saline was administered. The patients held their breath after Sonazoid injection. The real-time images were displayed in all the phases. Vessel flow in the lesion was visualized in the early vascular phase (about 10-40 s after Sonazoid administration) of the pulse subtraction harmonic imaging. Images were recorded and stored digitally in a cine-loop memory on a hard disk. The observers reviewed the images frame by frame from the stored images.

### Dynamic CT

Sixteen multidetector CT scanners (Aquilion 16; Toshiba) performed all the dynamic CT examinations, and the images were cephalocaudally obtained in 5-mm-thick sections at a pitch of 0.94 after intravenous bolus injection of nonionic contrast material (90 mL of 300 mgI/dL; Iopamiron®, Bayer Schering Pharma, Osaka, Japan) via an antecubital vein. The scanning delay set for the arterial and equilibrium phases was 30 s and 150 s, respectively.

### Sonographer's Profile

All the sonographic procedures were performed by 2 skilled sonographers. One was accredited by the Japan Society of Gastroenterology, the Japan Society of Hepatology, and the Japan Society of Ultrasonics in Medicine, who had experience of more than 1900 cases of RF ablation. The other was accredited by the Japan Society of Gastroenterology, who had experience of more than 100 cases of RF ablation. Two sonographers independently diagnosed the lesions. A final diagnosis was decided by the agreement of the 2 sonographers.

### Statistical Analysis

Statistical evaluation was performed using the Mann-Whitney U test and Fisher's exact test. The level of significance was set at

**Table 1.** Clinical characteristics of the patients

Patients	
Total number of patients	22
Age (median: min-max)	75: 58-90
Sex (Male / Female)	16/6
Tumors	
Etiology (HBV/HCV/Alcohol)	2/15/5
Location (S1/S2/S3/S4/S5/S6/S7/S8)	2/2/1/1/1/6/3/6
Size (mm)	17: 7-68
Depth (mm)	67.5: 30-170

HBV: hepatitis B virus; HCV: hepatitis C virus; mm: millimeter

p<0.05. Statistical analyzes were performed using the StatView (SAS Institute, Cary, NC, USA) and EZR (Saitama Medical Center, Jichi Medical University, Japan) software (18,19).

**Ethics**

The study was planned in conformity with the Declaration of Helsinki. The Ethics Committee of Omori Red Cross Hospital approved the protocol of this study.

**RESULTS**

**Patients' Clinical Characteristics**

The clinical characteristics of the patients are summarized in Table 1. A total of 22 patients, including 16 males and 6 females with a median age of 75 years (range: 58-90 years) were enrolled in this study. The underlying liver diseases in these hepatocellular carcinoma patients included hepatitis-B-virus-associated liver disease (2 patients), hepatitis-C-virus-associated liver disease (15 patients), and alcoholic liver disease (5 patients). The tumors were located in S1 (2 patients), S2 (2 patients), S3 (1 patient), S4 (1 patient), S5 (1 patient), S6 (6 patients), S7 (3 patients), or S8 (6 patients) of the liver (20). The median tumor size was 17 mm (range: 7-68 mm). The median tumor depth on the US images was 67.5 mm (range: 30-170 mm).

**Lesions Detected by Conventional US**

While there were no differences in the age, sex, etiology, location, or tumor depth on the US images, a significant difference was noted with regard to the tumor size between the lesions detected and undetected by conventional US (Table 2).

**Lesions Detected by Sonazoid-Enhanced US**

While there were no differences in the age, sex, etiology, location, or tumor size on the US images, a significant difference with regard to the tumor depth was observed between the lesions detected and undetected by Sonazoid-enhanced US (Table 3).

**Evaluation of Diagnostic Tests**

Table 4 lists the evaluation results of the diagnostic tests. We evaluated the diagnostic ability of conventional US for the diagnosis of tumor residues after percutaneous RF ablation in comparison with that of contrast-enhanced CT, and the results were as follows: apparent prevalence of 0.773 (95% confidence interval (CI): 0.546-0.922), true prevalence of 1.000 (95% CI: 0.781-1.000), sensitivity of 0.773 (95% CI: 0.546-0.992), specificity of NaN (95% CI: 0-1), positive predictive value of 1.000 (95% CI: 0.727-1.000), negative predictive value of 0 (95% CI: 0-0.614), and diagnostic accuracy of 0.514 (95% CI: 0.392-0.636).

Further, we evaluated the diagnostic ability of Sonazoid-enhanced US for the diagnosis of tumor residue after percutaneous RF ablation as compared to that of contrast-enhanced CT and the results were as follows: apparent prevalence of 0.864 (95% CI: 0.651-0.971), true prevalence of 1.000 (95% CI: 0.781-

**Table 2.** Clinical characteristics of the patients with lesions detected by conventional US

	Detected lesions n=17	Not detected lesions n=5	p
Age	77: 85-90	73: 61-86	0.6037*
Sex (Male/Female)	11/6	5/0	0.2663**
Etiology (HBV/HCV/Alcohol)	1/13/3	1/2/2	0.2937***
Location (S1/S2/S3/S4/S5/S6/S7/S8)	2/2/1/1/1/5/2/3	0/0/0/0/0/1/1/3	0.6700***
Size (mm)	16: 7-34	23: 17-68	0.0278**
Depth (mm)	65: 30-95	90: 60-170	0.0835**

\*Mann-Whitney U test; \*\*Fisher's exact test; \*\*\*Chi-square test. HBV: hepatitis B virus; HCV: hepatitis C virus; mm: millimeter

**Table 3.** Clinical characteristics of the patients with lesions detected by Sonazoid-enhanced US

	Detected lesions n=19	Not detected lesions n=3	p
Age	77: 58-90	68: 61-73	0.1643*
Sex (M/F)	13/6	3/0	0.5325**
Etiology (HBV/HCV/Alcohol)	1/15/3	1/0/2	0.0228***
Location (S1/S2/S3/S4/S5/S6/S7/S8)	2/2/1/1/1/6/2/4	0/0/0/0/0/0/1/2	0.6578***
Size (mm)	16: 7-98	19: 17-23	0.4428**
Depth (mm)	65: 30-95	110: 90-170	0.0109**

\*Mann-Whitney U test; \*\*Fisher's exact test; \*\*\*Chi-square test. HBV: hepatitis B virus; HCV: hepatitis C virus; mm: millimeter

1.000), sensitivity of 0.864 (95% CI: 0.651-0.971), specificity of NaN (95% CI: 0-1.000), positive predictive value of 1 (95% CI: 0.751-1.000), negative predictive value of 0 (95% CI: 0-0.806), and diagnostic accuracy of 0.864 (95% CI: 0.651-0.971).

Furthermore, when we evaluated the diagnostic ability of CO<sub>2</sub>-enhanced US for the diagnosis of tumor residue after percutaneous RF ablation as compared to that of contrast-enhanced CT, the results were as follows: apparent prevalence of 1.000 (95% CI: 0.781-1.000), true prevalence of 1.000 (95% CI: 0.781-1.000), sensitivity of 1.000 (95% CI: 0.781-1.000), specificity of NaN (95% CI: 0-1.000), positive predictive value of 1 (95% CI: 0.781-1.000), negative predictive value of NaN (95% CI: 0-1.000), and diagnostic accuracy of 1.000 (95% CI: 0.781-1.000).

**DISCUSSION**

Percutaneous radiofrequency ablation therapy has recently been established as a standard therapeutic technique. Tumor residue after percutaneous RF ablation is usually detected by contrast-enhanced CT. On the other hand, it is sometimes difficult to diagnose tumor residue by US devices. We compared the efficacy of contrast-enhanced CT with that of CO<sub>2</sub>-

**Table 4.** Apparent prevalence, sensitivity, and diagnostic accuracy of conventional US, Sonazoid-enhanced US, and CO<sub>2</sub>-enhanced US, with contrast-enhanced CT set as the gold standard

	Apparent prevalence	True prevalence	Se	Sp	PPV	NPV	Diagnostic accuracy
Conventional US (95% CI)	0.773 (0.546-0.922)	1.000 (0.781-1)	0.773 (0.546-0.922)	NaN (0-1)	1.000 (0.727-1)	0 (0-0.641)	0.773 (0.546-0.922)
Sonazoid enhanced US (95% CI)	0.864 (0.651-0.971)	1.000 (0.781-1)	0.864 (0.651-0.971)	NaN (0-1)	1.000 (0.751-1)	0 (0-0.0806)	0.864 (0.651-0.971)
CO <sub>2</sub> enhanced US (95% CI)	1.000 (0.781-1)	1.000 (0.781-1)	1.000 (0.781-1)	NaN (0-1)	1.000 (0.781-1)	NaN (0-1)	1.000 (0.781-1)

US: ultrasonography; CT: computed tomography; CI: confidence interval; Se: sensitivity; Sp: specificity; PPV: positive predictive value; NPV: negative predictive value; NaN: not a number

enhanced US, Sonazoid-enhanced US, and conventional US in detecting local residual tumor after percutaneous RF ablation therapy of hepatocellular carcinoma.

Many studies have suggested that Sonazoid-enhanced US is the most optimal method for the detection of local tumor residue after percutaneous RF ablation. However, few studies have evaluated the tumor depth in US images and the diagnostic difficulties associated with deep-seated lesions. This study revealed that CO<sub>2</sub>-enhanced US was superior to Sonazoid-enhanced US in detecting tumor residue after percutaneous RF ablation, especially sonographically deep-seated lesions.

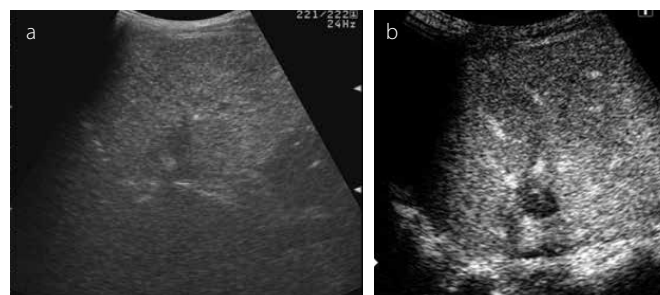
We describe 2 cases. We detected a tumor located 80 mm from the skin surface determined by both CO<sub>2</sub>-enhanced US (Figure 1a) and Sonazoid-enhanced US (Figure 1b). However, we also detected a tumor located 110 mm from the skin surface determined by CO<sub>2</sub>-enhanced US (Figure 2a), but remained undetected by Sonazoid-enhanced US (Figure 2b).

Table 2 shows that conventional US had a lower ability to detect large tumors as compared to contrast-enhanced CT. Thus, it may be necessary to combine multiple imaging modalities for evaluating the outcomes of hepatocellular carcinoma treatment.

The reason that a significant difference was noted in relation to the tumor size between the lesions detected and undetected by conventional US was unclear. The scan range of conventional US probe would possibly be unsuitable for a large tumor residue.

There were some limitations of this study: first, the study design was retrospective. Sample bias could have easily occurred; it is possible that we entered patients with tumors that were easy to detect by US. Second, the evaluation results by US are subjective and are affected by the sonographer's experience and technique. Third, the sample size was too small and beta errors may have occurred.

In conclusion, although CO<sub>2</sub>-enhanced US requires angiography, it was superior to Sonazoid-enhanced US and conven-



**Figure 1. a. b.** A tumor located 80 mm from the skin surface determined by both CO<sub>2</sub>-enhanced US (a) and Sonazoid-enhanced US (b)

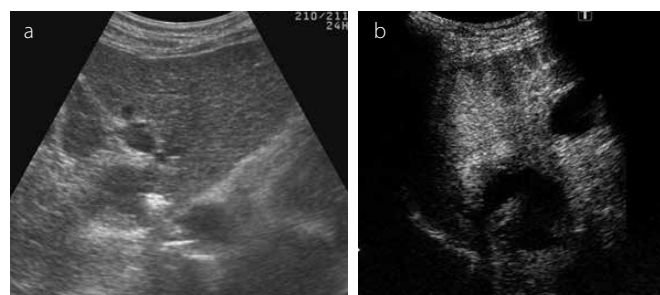


**Figure 2. a. b.** A tumor located 110 mm from the skin surface detected by CO<sub>2</sub>-enhanced US (a), but remained undetected by Sonazoid-enhanced US (b)

tional US in detecting tumor residues, especially deep-seated lesions, after percutaneous RF ablation. Further investigation without the limitations of the current study may be needed in the future.

**Ethics Committee Approval:** Ethics committee approval was received for this study from the ethics committee of Omori Red Cross Hospital.

**Informed Consent:** Written informed consent was obtained from patients who participated in this study.

**Peer-review:** Externally peer-reviewed.

**Author Contributions:** Concept - J.H., T.G.; Design - J.H., M.I.; Supervision - T.G., S.M.; Resources - T.G., S.N., S.S., T.I., T.M., H.O.; Materials - J.H., T.G.; Data Collection and/or Processing - J.H., T.G.; Analysis and/or Interpretation - J.H., M.I.; Literature Search - J.H., T.G., S.N., S.S., T.I., T.M., H.O., M.I., S.M.; Writing Manuscript - J.H., M.I.; Critical Review - T.G., S.N., S.S., T.I., T.M., H.O.; Other - M.I., S.M.

**Conflict of Interest:** No conflict of interest was declared by the authors.

**Financial Disclosure:** The authors declared that this study has received no financial support.

## REFERENCES

1. Altekruse SF, Henley SJ, Cucinelli JE, McGlynn KA. Changing hepatocellular carcinoma incidence and liver cancer mortality rates in the United States. *Am J Gastroenterol* 2014; 109: 542-53. [\[CrossRef\]](#)
2. Metts J, Carmichael L, Kokor W, Scharffenberg R. Hepatitis C: prevalence, transmission, screening, and prevention. *FP Essent* 2014; 427: 11-7.
3. Lin S, Hoffmann K, Schemmer P. Treatment of hepatocellular carcinoma: a systematic review. *Liver Cancer* 2012; 1: 144-58. [\[CrossRef\]](#)
4. Lee DH, Lee JM, Lee JY, et al. Radiofrequency ablation of hepatocellular carcinoma as first-line treatment: long-term results and prognostic factors in 162 patients with cirrhosis. *Radiology* 2014; 270: 900-9. [\[CrossRef\]](#)
5. Matsuda Y, Yabuuchi I. Hepatic tumors: US contrast enhancement with CO<sub>2</sub> microbubbles. *Radiology* 1986; 161: 701-5. [\[CrossRef\]](#)
6. Leen E, McArdle CS. Ultrasound contrast agents in liver imaging. *Clin Radiol* 1996; 51: 35-9.
7. Harvey CJ, Blomley MJK, Eckersley RJ, Cosgrove DO. Developments in ultrasound contrast media. *Eur Radiol* 2001; 11: 675-89. [\[CrossRef\]](#)
8. Numata K, Luo W, Morimoto M, et al. Contrast enhanced ultrasound of hepatocellular carcinoma. *World J Radiol* 2010; 2: 68-82. [\[CrossRef\]](#)
9. Akiyama T, Inamori M, Saito S, et al. Levovist ultrasonography imaging in intracystic hemorrhage of simple liver cyst. *World J Gastroenterol* 2008; 14: 805-7. [\[CrossRef\]](#)
10. Shirato K, Morimoto M, Tomita N, et al. Hepatocellular carcinoma: therapeutic experience with percutaneous ethanol injection under real-time contrast-enhanced color Doppler sonography with the contrast agent Levovist. *J Ultrasound Med* 2002; 21: 1015-22. [\[CrossRef\]](#)
11. Luo W, Numata K, Morimoto M, et al. Clinical utility of contrast-enhanced three-dimensional ultrasound imaging with Sonazoid: findings on hepatocellular carcinoma lesions. *Eur J Radiol* 2009; 72: 425-31. [\[CrossRef\]](#)
12. Shiozawa K, Watanabe M, Takayama R, et al. Evaluation of local tumor residue after treatment for hepatocellular carcinoma by contrast-enhanced ultrasonography using Sonazoid: comparison with dynamic computed tomography. *J Clin Ultrasound* 2010; 38: 182-9.
13. Marone G, Francica G, D'Angelo V, et al. Echo-guided radiofrequency percutaneous ablation of hepatocellular carcinoma in cirrhosis using a cooled needle. *Radiol Med* 1998; 95: 624-9.
14. Kirikoshi H, Saito S, Yoneda M, et al. Outcome of transarterial chemoembolization monotherapy, and in combination with percutaneous ethanol injection, or radiofrequency ablation therapy for hepatocellular carcinoma. *Hepatol Res* 2009; 39: 553-62. [\[CrossRef\]](#)
15. Livraghi T, Goldberg SN, Lazzaroni S, Meloni F, Solbiati L, Gazelle GS. Small hepatocellular carcinoma: treatment with radiofrequency ablation versus ethanol injection. *Radiology* 1999; 210: 655-61. [\[CrossRef\]](#)
16. Inoue T, Minami Y, Chung H, et al. Radiofrequency ablation for hepatocellular carcinoma: assistant techniques for difficult cases. *Oncology* 2010; 78(Suppl 1): 94-101. [\[CrossRef\]](#)
17. Miyamoto N, Hiramatsu K, Tsuchiya K, Sato Y. Carbon dioxide microbubbles-enhanced sonographically guided radiofrequency ablation: treatment of patients with local progression of hepatocellular carcinoma. *Radiat Med* 2008; 26: 92-7. [\[CrossRef\]](#)
18. Kanda Y. Investigation of the freely available easy-to-use software 'EZR' for medical statistics. *Bone Marrow Transplant* 2013; 48: 452-8. [\[CrossRef\]](#)
19. Kikkawa N, Inamori M, Inoue S, et al. Comparative Study of the QUEST Questionnaire and GerdQ Questionnaire for Japanese students. *Hepatogastroenterology* 2014; 61: 1605-10.
20. Couinaud C. Liver anatomy: portal (and suprahepatic) or biliary segmentation. *Dig Surg* 1999; 16: 459-67. [\[CrossRef\]](#)